Materials and Design 191 (2020) 108629

Contents lists available at ScienceDirect

Materials and Design

journal homepage: www.elsevier.com/locate/matdes

One-step synthesis of sandwich-type Cu/graphene/Cu ultrathin foil with enhanced property via electrochemical route

Gongsheng Song [a,b,c], Qing Wang [c], Li Sun [a], Sishi Li [a,b], Yafei Sun [e,*], Qiang Fu [d], Chunxu Pan [a,b,d,**]

[a] School of Physics and Technology, MOE Key Laboratory of Artificial Micro- and Nano-structures, Wuhan University, Wuhan 430072, China
[b] Suzhou Institute of Wuhan University, Suzhou 215123, China
[c] Department of Engineering, Durham University, Durham DH1 3LE, United Kingdom
[d] Center for Electron Microscopy, Wuhan University, Wuhan 430072, China
[e] School of Intelligent Manufacturing and Equipment, Shenzhen Institute of Information Technology, Shenzhen 518172, China

HIGHLIGHTS

- The Cu/Gr/Cu ultrathin foil is synthesized by one-step electrochemical route.
- Cu is deposited successively on substrate and GO under different over-potentials.
- The foil is of thickness as thin as 4–5 μm and twice tension strength enhancement.
- The high performances are attributed to strong interface bonding and graphene.
- This work can also be used to other metal/Gr/metal layered composites.

GRAPHICAL ABSTRACT

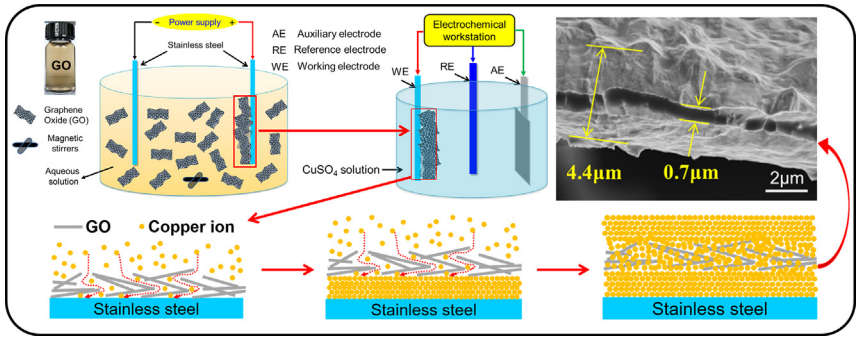

ARTICLE INFO

Article history:
Received 21 November 2019
Received in revised form 3 March 2020
Accepted 4 March 2020
Available online 10 March 2020

Keywords:
Electrochemical synthesis
Ultrathin copper foil
Graphene
Tensile strength
Layered composite

ABSTRACT

A layered structure has a better effect on improving performance of the graphene-reinforced composites due to its unique two-dimensional structure and excellent properties. In this paper, a novel "one-step" electrochemical route was proposed for synthesizing the graphene-reinforced ultrathin copper (Cu) foil with high performance. The process includes: 1) A loose graphene oxide (GO) membrane, was prepared by electrophoresis deposition (EPD), that allows Cu ions passing through; 2) According to the difference of Cu deposition potential on different substrates, a potential step was designed for electrodepositing Cu successively on both sides of the GO membrane, i.e., the bottom Cu layer forms under low over-potential, while the top Cu layer forms under high over-potential. The experimental results show that the foil thickness reaches to as thin as 4–5 μm, and the tensile strength is almost twice as large as that of pure Cu foil. The process is simple, controllable and possible mass production, and expected to further practical applications in fields of Cu clad plate, printed circuit board and lithium-ion battery cathode collector system for saving raw material and also the space. In addition, this work proposes a new idea for preparing the layered composites via electrochemical route.

* Corresponding author.
** Correspondence to: C. Pan, School of Physics and Technology, MOE Key Laboratory of Artificial Micro- and Nano-structures, Wuhan University, Wuhan 430072, China.
E-mail addresses: sunyf@sziit.edu.cn (Y. Sun), cxpan@whu.edu.cn (C. Pan).

https://doi.org/10.1016/j.matdes.2020.108629

1. Introduction

As an important raw material, electrolytic copper (Cu) foil has been widely used in areas, such as Cu clad plate (CCL), printed circuit board (PCB), and lithium ion battery cathode collector system [1]. For instance, in lithium ion battery, Cu foil is not only the carrier of negative electrode, but also acts as the electron collection and conduction [2]. In commercial applications, to produce ultrathin Cu foil with high-strength and high-conductivity is still a challenge [3]. In general, ultrathin copper foil is defined as thickness of <12 μm [4]. In order to improve its performance, many strategies have been proposed including optimizing the electrodeposition process [5] and adding nano-reinforcements, such as Si_3N_4 [6], graphite, [7] carbon nanotubes, [8,9] graphene [10,11], and so on.

As a two-dimensional planar structure of a single atomic layer of carbon, Graphene (Gr) is of a theoretical thickness 0.35 nm and its carbon atoms are all tightly connected with each other in the form of sp^2 hybridization. Therefore, Gr each lattice consists of a stable hexagonal structure formed by three sigma bonds, which results in unique properties, such as carrier mobility reach up to 200,000 $cm^2/(V \cdot s)$ at room temperature [12,13], and tensile strength up to 130 GPa and elastic modulus to 1.1 TPa. In addition to broad application prospects in the fields of microelectronics, energy, information and so on, Gr is especially considered to be an ideal reinforcement in composites [14–16].

In recent years, high performance Cu-Gr composites prepared by electrochemical deposition have attracted much attentions [17–19]. The basic approach is to add Gr or GO or its derivatives into the electrolyte, and treats it with ultrasound or surfactant for uniform dispersion. And then the co-deposition of copper and graphene are occurred on the cathode under electrical current to form a film or coating. Table 1 lists the summary of researches on Cu-based composites containing Gr and carbon nanotubes (CNTs). Obviously, the Gr co-deposition greatly increases the mechanical properties of Cu foil, and also makes its electrical conductivity slightly improve or remains unchanged. In comparison, some work on layered Cu-carbon nanocomposite films exhibit better enhancing effect on mechanical properties, such as up to 1.5 GPa compressive strength. The ultra-high strengths of the Cu-Gr nanolayered structures indicate the effectiveness of graphene in blocking dislocation propagation across the Cu-Gr interface [22]. Besides, Yi et al. [23] prepared a sandwich structural CNTs/Cu/CNTs composite, where a template method was used for preparing the freestanding CNTs network film. Then, using the film as the cathode, two anodic electrodes were applied during electrodeposition, so that the electrodeposition could occur simultaneously on both sides of the CNTs film.

In generally, commercial Cu foil is divided into several thickness ranges, i.e., thick foil (>70 μm), conventional foil (18 μm–70 μm), thin foil (12 μm–18 μm) and ultrathin foil (<12 μm), respectively [25]. And, the tensile strength is around 350 MPa. Therefore, the value higher than 400 MPa is called the high-performance Cu foil.

Obviously, because of low strength, the ultrathin foil is prone to wrinkle and tearing, which make its production, transportation and application very difficult. At present, the carrier method is adopted to prepare the ultrathin Cu foil in industry, which refers to a process, i.e., deposit the ultrathin Cu foil firstly on a thick Cu foil, and then peels it off [26]. Obviously, the operation of this process is tedious and the industrial production cost is high, meanwhile the performance of the ultrathin Cu foil has not been improved.

Electrophoretic deposition (EPD) is a surface treatment technology that has been widely used in processing advanced ceramics and coatings. In brief, EPD is a process for depositing charged colloidal particles on electrode under electric field. By using EPD technology many researches prepared the dense GO films as corrosion resistant coatings [27–30].

This paper proposed a novel process to prepare the layered Cu/Gr/Cu composite foil, i.e., according to the difference of Cu deposition potential on different substrates, a potential step was designed for electrochemical deposition, which achieved the one-step preparation of the Cu/Gr/Cu ultrathin foil, as shown in Fig. 1. The foil's thickness reached to as thin as 4–5 μm and had a twice tension strength enhancement, which was firstly reported. The process is of advantages, such as simple and controllable, and expects to further mass production in industry. Further practical applications are expected in the areas, such as the Cu clad plate (CCL), printed circuit board (PCB), and lithium ion battery cathode collector system for saving row material and also the space. In addition, this work provides a new idea for preparing the layered composites via electrochemical route.

2. Experimental section

2.1. Preparation of the EPD-GO film

All experimental reagents were in analytical grades, and deionized water was utilized to prepare the electrolyte. Fig. 1 illustrates the preparation process of the Sandwich-type Cu/Gr/Cu ultrathin foil. The detailed process for preparing the EPD-GO film was as follows:

1) Graphene oxide (GO) was synthesized from natural graphite powders by a modified Hummers' method and the detailed process operations was described in supporting information.
2) GO was first dispersed in deionized water and sonicated for 10 min at room temperature. A uniform and stable aqueous solution containing 0.5 $mg \cdot ml^{-1}$ of GO was obtained.
3) A direct current (DC) electrophoresis method was used by using a DC power supply (KXN-3010D, Zhaoxin, China). Both the cathode and anode were Type 304 stainless steel with a size of 30 mm * 50 mm * 0.5 mm and the applied voltage was fixed at 5 V, while the electrophoresis time varied from 10 s to 60 s.
4) A hydrous EPD-GO film was obtained on the anode and dried in the air for later use. This loose film allowed Cu ions to permeate through and contacted with the stainless steel substrate.

2.2. Preparation of the Sandwich-type Cu/Gr/Cu layered composite foil

In view of the difference of the Cu deposition potential on different substrates, a potential step method in a three-electrode system was

Table 1
A site view on carbon nanomaterials reinforced copper-based composites.

Composition	Method	Thickness (μm)	Properties (compared with Cu foil)	Ref.
Cu-Gr	DCED	20	Tensile strength, hardness and elastic modulus of the Cu-Gr foil increased by 35%, 42% and 33%, respectively.	[18]
Cu-Gr	PRED	12	Young's modulus, yield strength and tensile strength of the Cu-Gr foil increased by 17%, 39.1% and 21.1%, respectively	[20]
Cu-Gr	PRED	30	Hardness and elastic modulus of the Cu-Gr foil increased by 96% and 30%	[21]
Multi-layer (Cu/graphene)	CVD single graphene	3	1.5 GPa compressive strength	[22]
Sandwich-tye CNTs/Cu/CNTs	DCED with a template method	10–30	Electrical conductivity of the composite prepared in BAPB up to 2.02×10^5 S cm^{-1}.	[23]
Laminated (CNT/Cu)	Dip-Coating	7.5	(Cu/CNTs) 2 Cu nanocomposites show 45% higher yield strength	[24]

Note: Gr is graphene, CNTs is carbon nanotubes, DCED is direct current electrodeposition, PRED is pulse reverse electrodeposition, CVD is chemical vapor deposition.

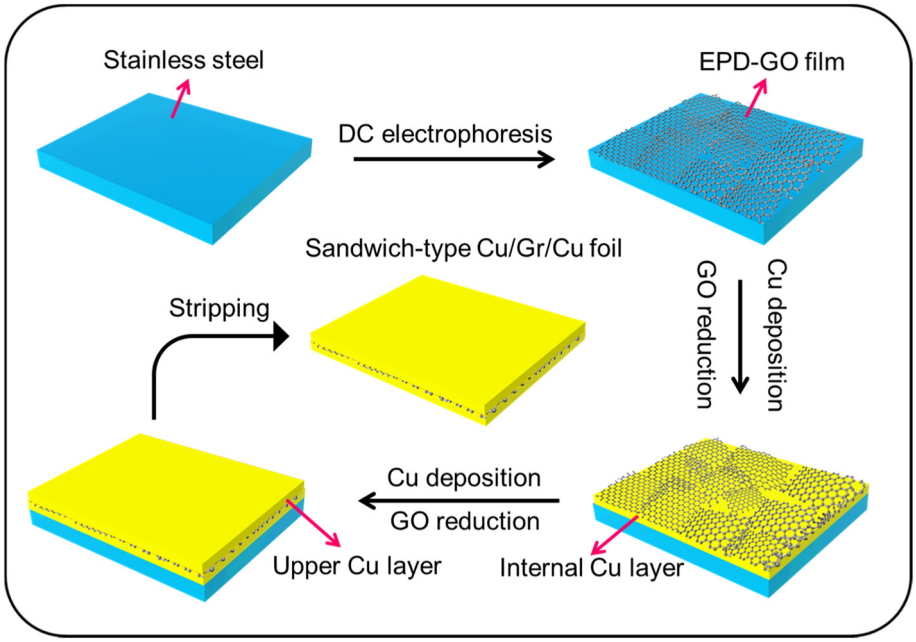

Fig. 1. Schematic diagram of preparation of the sandwich-type Cu/Gr/Cu ultrathin foil.

designed for preparing the sandwich-type Cu/Gr/Cu foil by using an electrochemical workstation (CHI660E, Chenhua, China). The system consisted of a platinum foil with a large area, a mercury/mercuric sulfate (Hg/Hg_2SO_4) as the counter electrode, and a reference electrode. As shown in Fig. 2, the process was performed in an electrolyte consisting of 100 $g \cdot L^{-1}$ $CuSO_4$, 30 $g \cdot L^{-1}$ H_2SO_4, and the specific steps were: 1) had a thin EPD-GO film on the SS substrate; 2) carried out electrochemical deposition at a low overpotential (−0.55 V vs. Hg/Hg_2SO_4) to allow Cu ions passing through the GO film and get to SS substrate to form the bottom Cu layer; 3) Shift to a high overpotential (−0.65 V vs. Hg/Hg_2SO_4) to obtain the top Cu layer. In general, the Cu/Gr/Cu ultrathin foil could be stripped directly from the stainless steel substrate due to the inferior adhesive property, which was similar to the continuous production in industry. It also described in our previous work [20]. The foil samples were blown dry by hair drier for the subsequent characterizations and tests. For comparison, pure Cu foil was also prepared by using the same method.

2.3. Characterizations

The morphologies and chemical compositions of the GO and the foil samples were characterized using several analysis instruments, including a scanning electron microscope (SEM) (S-4800, Hitachi, Japan, and SIRON, FEI, The Netherlands) equipped with an energy-dispersive X-ray spectroscopy (EDS); a transmission electron microscope (TEM) (JEM-2100, JEOL, Japan), with the acceleration voltage of 200 kV; a Fourier transform infrared spectrometer (FT-IR, Nicolet iS10, Thermo Fisher, USA) with a scanning range of 525–4000 cm^{-1} and a laser scanning confocal micro-Raman spectrometer (Raman) (LabRAM HR, HORIBA, France) with a laser excitation wavelength of 488 nm and scans with an extended range of 1000–3000 cm^{-1}.

Absorbance of GO was measured by using a diffuse reflectance spectra of a UV–vis spectrophotometer (UV-2550; Shimadzu, Kyoto, Japan) in absorption mode, in which deionized water was used as a background between 190 nm and 800 nm scopes.

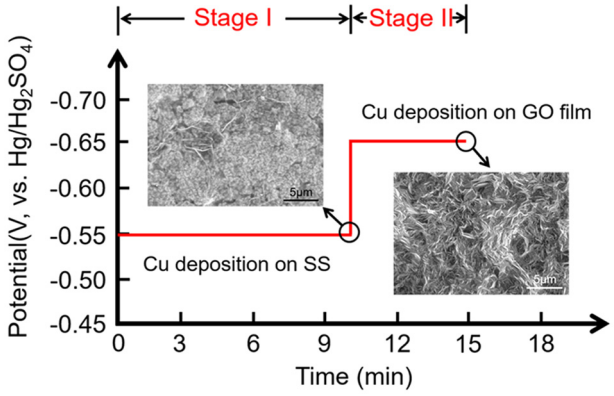

Fig. 2. Schematic diagram of the potential step method with corresponding SEM morphologies.

2.4. Property measurements

The tensile strength of the samples was measured by an electronic universal testing machine (model CMT6203, MTS systems Co., Ltd.) in accordance with the testing method IPC-TM-650, where the foil width was 12.7 mm and tensile rate was 2 $mm \cdot min^{-1}$. After tensile test, the cross-section fracture surfaces were observed by using SEM. The Gr strengthening mechanism was expressed by the following equation [31,32]:

$$\sigma_c = \sigma_m + \Delta\sigma_{LT} + \Delta\sigma_D + \Delta\sigma_{GR} \quad (1)$$

where σ_c and σ_m were tensile strength of the composite and matrix, respectively. σ_{LT}, σ_D and σ_{GR} were the strengthening contributions from load transfer, dislocation strengthening and grain refinement, respectively. The square resistance of the foil samples was measured using a four-point probe instrument (RTS-9, 4 Probes Tech, China). The resistivity of all samples was calculated using the following equation:

$$\rho = d \cdot R_s \quad (2)$$

where ρ, d and R_s were resistivity, thickness and square resistance of the foils, respectively.

3. Experimental results

Fig. 3 shows the microstructural characterizations of GO. SEM and TEM observations revealed that GO was of a nearly transparent lamellar structure and crimped at the edges. The strong diffraction spots of selected-area electron diffraction (SAED) pattern demonstrated it a well-defined hexagonal structure, and high crystallinity [33]. The FT-IR spectrum showed the GO surface contained oxygen-containing functional groups [34], involving O—H (hydroxy) stretching vibration near 3190 cm^{-1}, C═O (carboxyl/carbonyl) stretching near 1719 cm^{-1}, C═C (aromaticring) near 1621 cm^{-1}, and C—O (alkoxy) stretching near 1043 cm^{-1}. These groups would improve the dispersion of GO in aqueous. The UV–vis spectra had a peak at 227 nm, which was due to $\pi \rightarrow \pi^*$ of C═C bond, and a shoulder at ~290–300 nm, corresponding to $n \rightarrow \pi^*$ transition of the C═O bond [35]. The Raman spectrum indicated it was a typical GO, i.e., D peak near 1360 cm^{-1} revealing the defect density due to the lattice vibration leaving the Brillouin zone center; G peak near 1586 cm^{-1} was caused by sp^2 hybridization of carbon atoms of in-plane vibration; 2D peak near 2700 cm^{-1} was the phonon resonance second-order Raman peak indicating the way of carbon atoms stack in graphene; and the scattering of D peak and 2D peak in the valley generates the D+ G peak near 2935 cm^{-1} [36–38].

Fig. 4 shows the SEM morphologies of the EPD-GO films with different durations. When the EPD time was short, the GO film exhibited a flat surface with fewer folds. The EDS element mapping, as shown in Fig. S1, also indicates that GO was successfully electrodeposited on the SS substrate. However, for the longer deposition time, the GO film became higher stack and fold significantly, due to the increased thickness.

Further, the compactness of the EPD-GO film was tested by measuring the open circuit potential (E_{ocp}) - time (T) curve and linear sweep voltammetry (LSV) curve in the copper sulphate electrolyte, respectively, as shown in Fig. 5. In general, the E_{ocp}-T curve is used to study

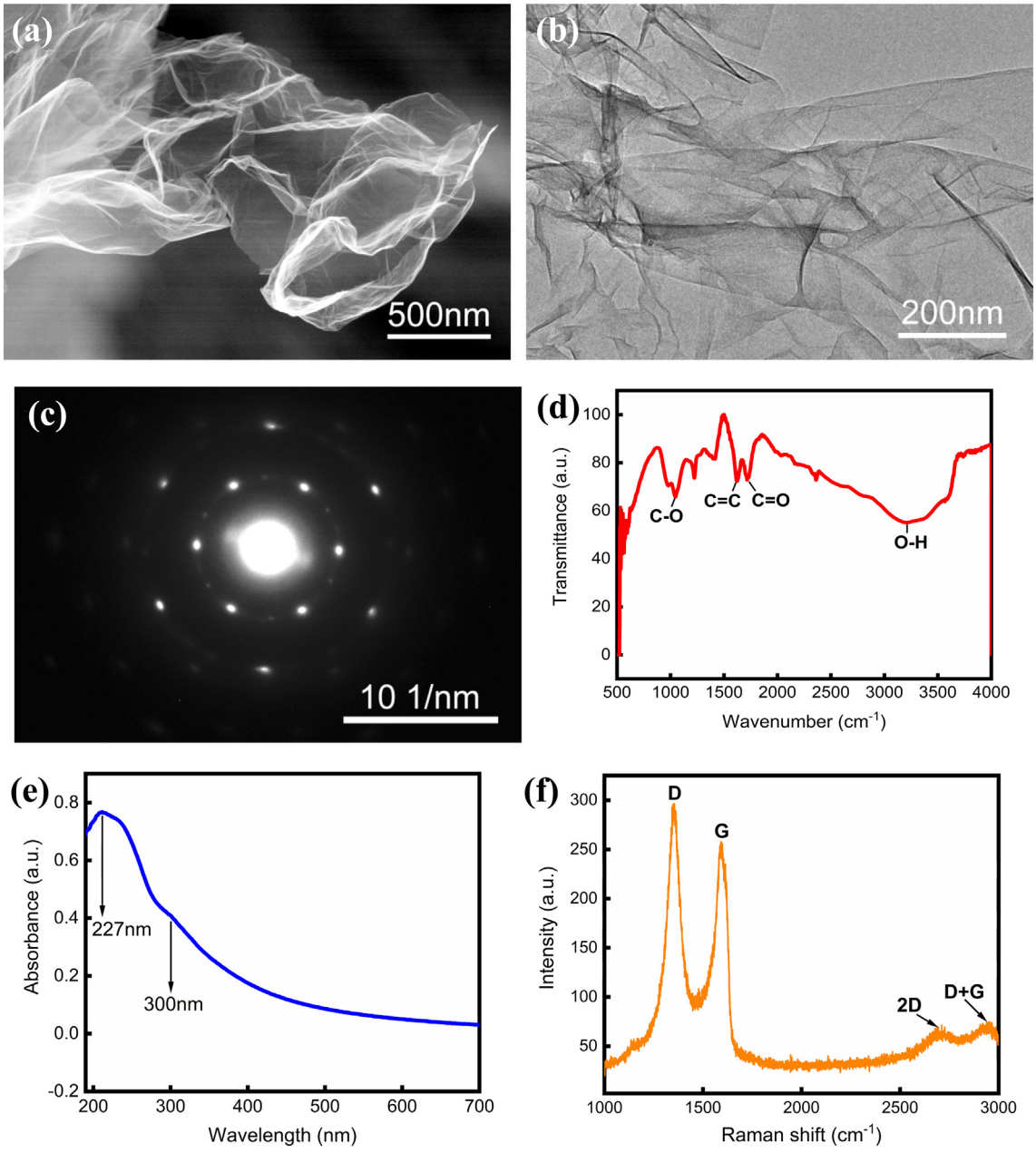

Fig. 3. Microstructural characterizations of graphene oxide (GO). (a) SEM morphology; (b) TEM micrograph; (c) SAED pattern of the sheet in (b); (d) FT-IR spectrum; (e) UV–vis spectrum; (f) Raman spectrum.

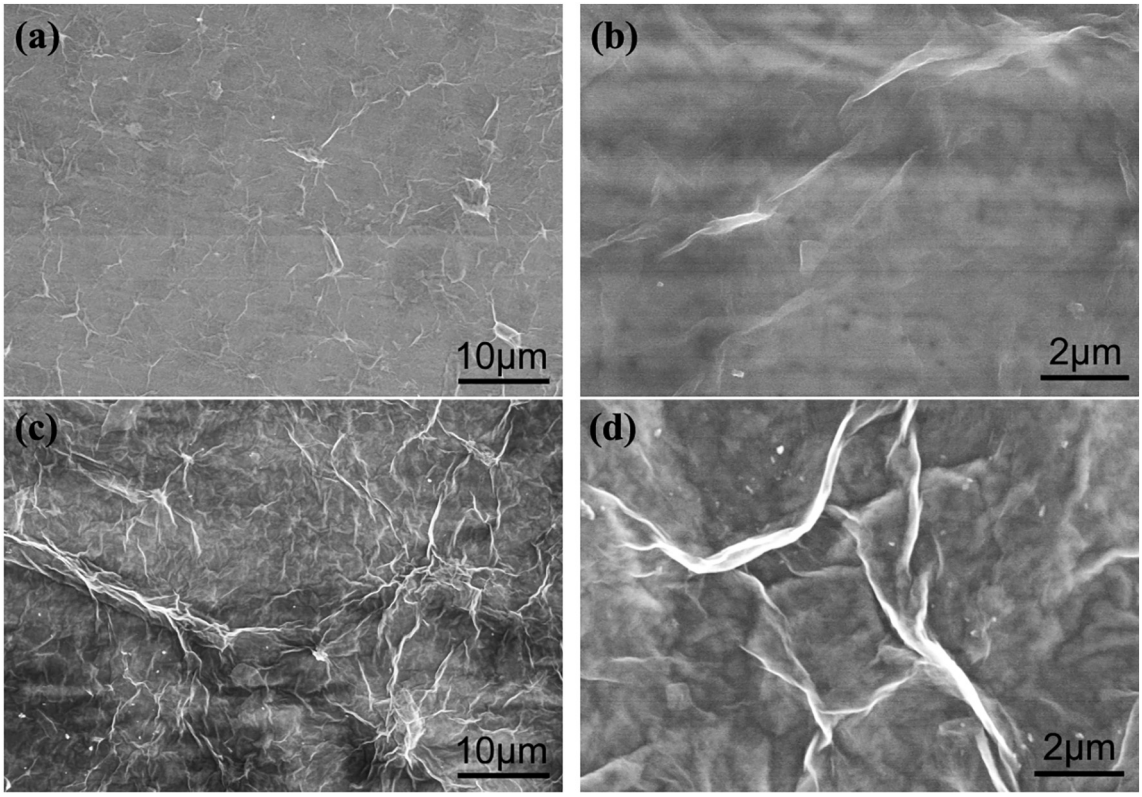

Fig. 4. SEM morphologies of the EPD-GO film with different durations. (a) electrophoresis for 10 s; (b) high magnification; (c) electrophoresis for 60 s; (d) high magnification.

the sensitivity of the interaction between working electrode and electrolyte as well as the probability of corrosion reaction. The more negative the E_{ocp}, the stronger the action, and the stronger corrosion. In the present case, as shown in Fig. 5 (a), E_{ocp} of the EPD-GO film varied from the positive potential close to the freestanding GO film to the negative potential of the SS as time increasing, which revealed that the electrolyte could pass through the EPD-GO film and interacted with the SS substrate. Similarly, Cu ions exhibited different deposition potentials on SS, EPD-GO and freestanding GO film, as shown in Fig. 5(b). Therefore, these results provided a possibility to prepare the Cu/Gr/Cu layered foil by using such an uncompact EPD-GO film.

Fig. 6 shows the SEM surface morphologies of the bottom Cu layer. As the deposition time increased, the Cu deposition on the SS surface continuously took place and became more and more compact, and eventually formed a thin Cu layer. The EDS elements mapping also confirmed the Cu deposition growth on the SS substrate, as shown in Figs. S2 and S3. In addition, the Cu surface showed a good appearance, as shown in Fig. 6(g), and the portion within the black dotted frame will be used for cross-section observation after tensile test, As shown in Fig. 6(h).

Numerous studies have demonstrated that GO can be reduced to reduced GO (or Gr) during electrochemical deposition. In the present work, from Raman spectra (Fig. S4), it could be seen that the peak strength ratio (I_D/I_G) of the Gr in the Cu/Gr/Cu foil decreased significantly, when compared with the EPD-GO film, which indicated that GO was reduced to Gr during the foil preparation.

In addition, in order to observe the Sandwich structure more clearly under SEM, two kinds of composite foils with different Gr interlayers thickness were prepared, i.e., the Cu/Gr1/Cu foil with thinner Gr interlayer, and the Cu/Gr2/Cu foil with relatively thicker Gr interlayer. Fig. 7 shows the EDS elemental mappings of the cross-sectional Cu/Gr2/Cu foil. The Sandwich structure was clearly observed and the Gr

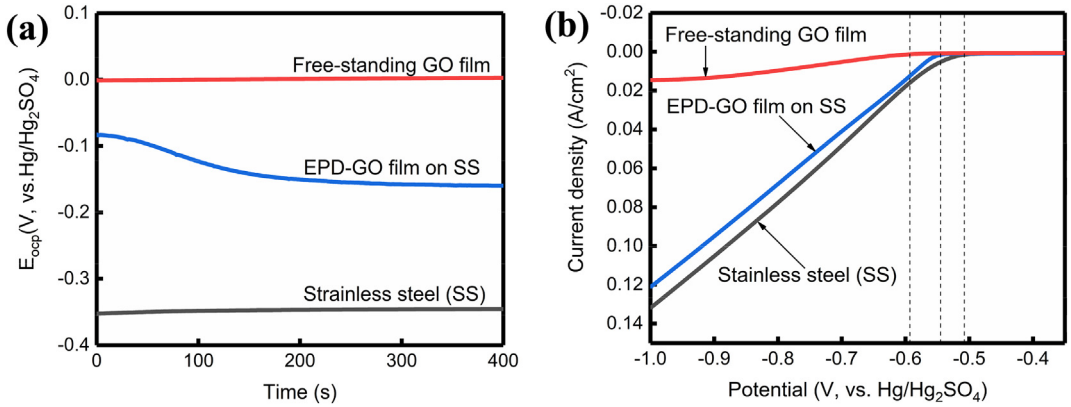

Fig. 5. (a) E_{ocp} - T curves; (b) linear sweep voltammetry curves.

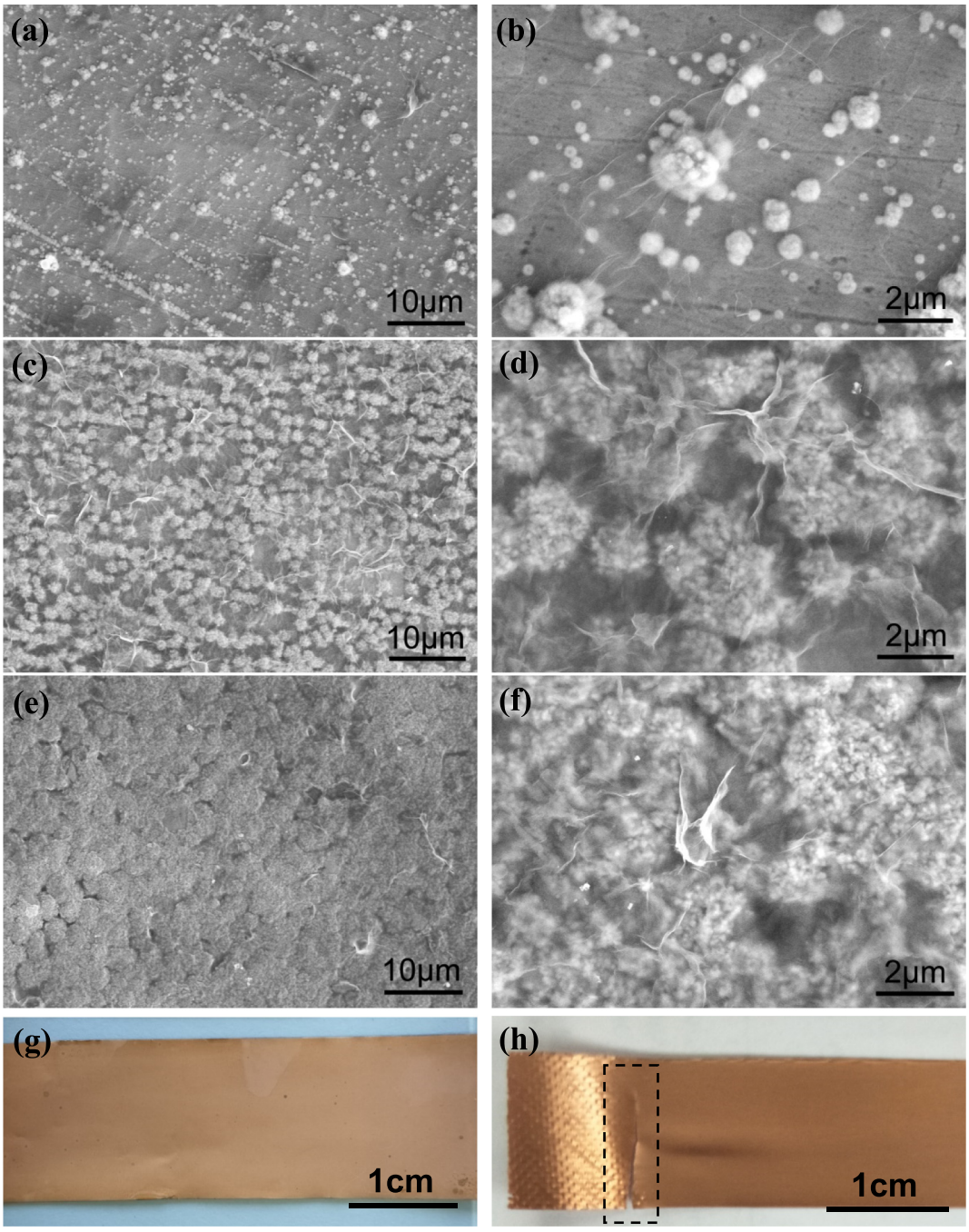

Fig. 6. SEM morphologies of the bottom Cu layer obtained with different deposition time at different magnifications; (a) and (b) 1 min; (c) and (d) 5 min; (e) and (f) 10 min; (g) general view of the foil; (h) foil after tensile test.

thickness was about 0.7 μm. The presence of O element was attributed to the cuprous oxide formation during electrodeposition.

Fig. 8 shows the SEM morphologies of the foils' tensile fracture surfaces. It could be seen that the total foil thickness was about 4.2–4.5 μm including the Gr interlayer < 0.7 μm, which was much less than the thickness 10 μm of commercial ultrathin foil, while in Fig. 8 (b), the Gr interlayer was too thin to be observed. In addition, from the top view, the edges of the pure Cu foil fracture surface were relatively flat, while the two composite foils showed jagged and tearing edges, which indicated a high ductility and strong interface bonding strength between Gr and Cu [39–41]. Fig. S4 shows the Raman peak of Cu_2O, which again confirmed the Cu oxidation during electrodeposition process. This result was also consistent with other researchers [42,43].

Fig. 9 illustrates the test results of tensile strength and electrical properties of the different foils. Obviously, compared with pure Cu foil (270 MPa), the Cu/Gr1/Cu foil with thinner Gr interlayer exhibited the highest tensile strength up to 535 MPa, i.e., almost double the value. In regarding to the electrical conductivity of the foils, the resistivity was calculated by using the following equation:

$$\rho = d \cdot R_s \tag{3}$$

where ρ is the resistivity, d is the thickness and R_s is the square resistance. As shown in Fig. 9 (b), the resistivities of the Cu/Gr1/Cu foil with thinner Gr interlayer and pure Cu foil were comparable, but the

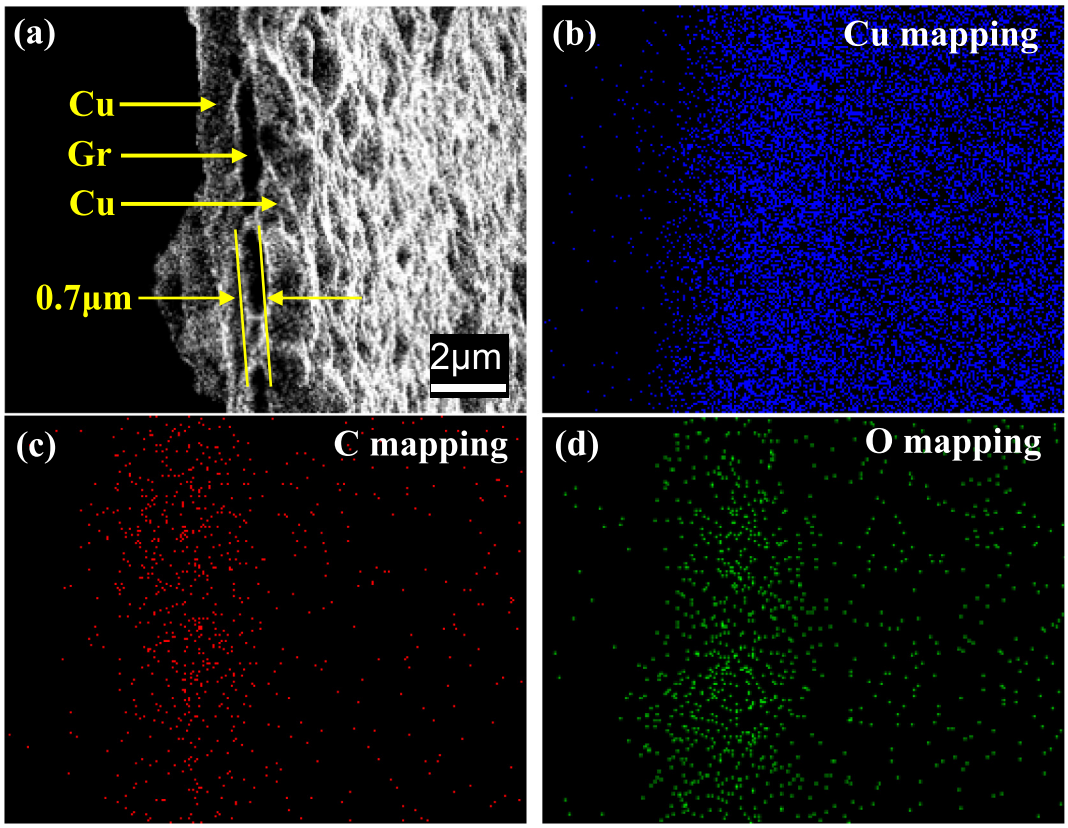

Fig. 7. Cross-sectional EDS elemental mappings of the Cu/Gr/Cu foil. (a) SEM image; (b) Cu element; (c) C element; (d) O element.

Cu/Gr2/Cu foil with relatively thicker Gr interlayer increased significantly.

4. Discussion

In general, there are three possible strengthening mechanisms accounting for the enhanced strength of the metal - Gr composites, i.e., load transfer strengthening [44], dislocation strengthening [22] and grain refinement [21], and it can be expressed by the following equation [31,33]:

$$\sigma_c = \sigma_m + \Delta\sigma_{LT} + \Delta\sigma_D + \Delta\sigma_{GR} \quad (4)$$

where σ_c and σ_m represent tensile strength of the composite and matrix, respectively; σ_{LT}, σ_D and σ_{GR} are the strengthening contributions from load transfer, dislocation strengthening and grain refinement, respectively.

For the Sandwich-type Cu/Gr2/Cu layered composite foil, the strengthening effect of was proposed to the following mechanism:

1) Effective load transfer is the most important strengthening mechanism, due to Gr large specific surface area and high aspect ratio, and the load transfer efficiency depends on the interfacial bonding strength. In the present work, such interface was built by the formation of Cu-O-C bonding during electrodeposition, which not only strengthened the load transfer effect, but also fully utilized the intrinsic performance of Gr.
2) Dislocation strengthening effect. Many studies indicated that Gr played a barrier to block dislocation slip [32,45], which caused the high dislocation density at the interface.
3) Grain refinement effect. In our previous work, it was demonstrated that Gr provided more active sites for metal electrodeposition, which hindered the growth of metal crystal nucleus, and resulted in the refined grains [21,46].

However, for the Cu/Gr2/Cu foil with thick Gr interlayer, the tensile strength decreased obviously, as shown in Fig. 9(a), which could be attributed to the impeding of the Cu ions penetration through the thicker Gr layers. Therefore, the top Cu layer would quickly nucleate and grow under high overpotential and further hindered the Cu ions penetration. Alternatively, the GO film failed to form a strong interface bonding with Cu. The detailed mechanism was schematically illustrated in Fig. 10. Additionally, Fig. S5 also confirmed this mechanism.

Regarding electrical property of the Sandwich-type Cu/Gr/Cu layered composite foil, the resistance comes mainly from three factors, i.e., Cu, Gr and the Cu/Gr interface [47–49]. Obviously, the resistance of Cu is fixed, and therefore, the final variation determined by the other two factors, i.e., reduction degree of GO into Gr during electrodeposition and the Cu/Gr interfacial resistance. In general, the dense transition layer is in favor of higher electrical conductivity, while the loose one tends to hinder the electron conduction in composites [50,51]. Consequently, for the present samples, the thinner Gr interlayer was of a strong bonding interface between Cu and Gr, which would result in small resistivity, while the relatively thicker Gr interlayer had a higher resistivity due to the loose Gr structure. This phenomenon could also be interpreted diagrammatically from Fig. 10.

5. Conclusions

In order to challenge the mass production of ultrathin Cu foil in industry, a new electrochemical route is proposed to synthesize a kind of Sandwich-type Cu/Gr/Cu layer composite foil, regarding Gr's strong mechanical and electrical properties.

1) The “one-step” preparation process is based upon two principles, i.e., the loose GO film from EPD method allows Cu ions penetration, and there are different Cu deposition potentials on different

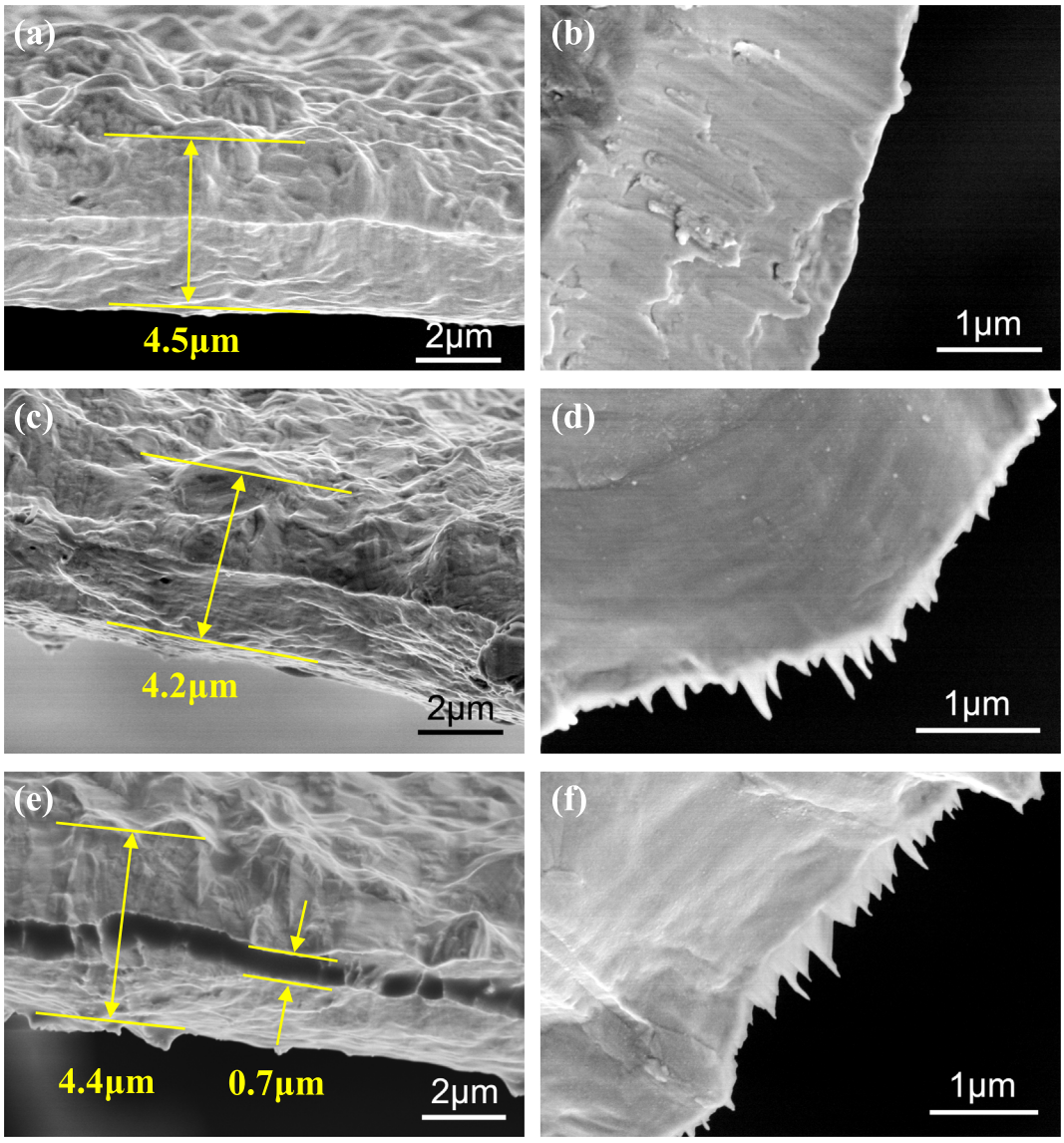

Fig. 8. Lateral view of fracture SEM morphologies of the foil fractural surfaces after tensile test. (a) and (b) pure Cu foil; (c) and (d) Cu/Gr1/Cu foil; (e) and (f) Cu/Gr2/Cu foil.

substrates. Therefore, the bottom Cu layer forms during low potential step, while the top Cu layer forms during high potential step.

2) By adjusting the electrodeposition time and using thinner GO film, the thickness of the Cu/Gr/Cu foil can reaches to as thin as 4–5 μm, and comparing to pure Cu foil, it tensile strength increases to almost twice value, while the electrical conductivity is basically unchanged.
3) This process is of advantages, such as simple, controllable and possible large-scale production in industry. It is expected to be broadly

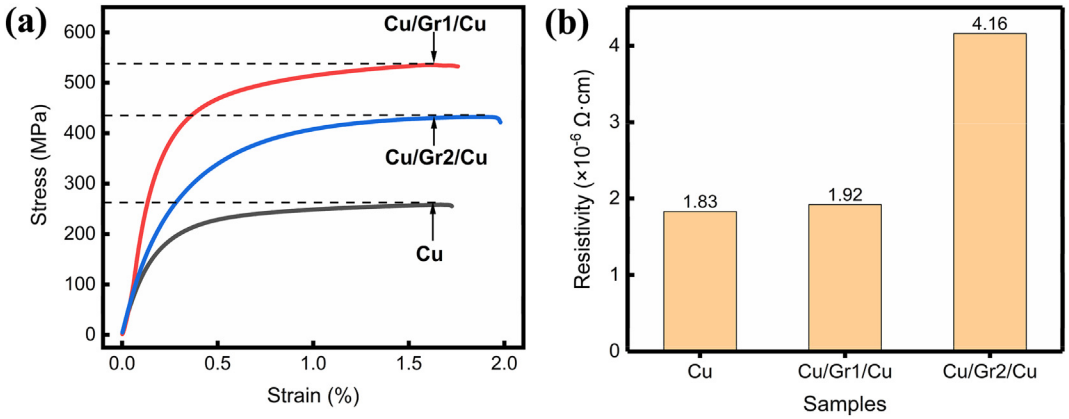

Fig. 9. Mechanical and electrical properties of the foils. (a) Stress-stain curves; (b) resistivity.

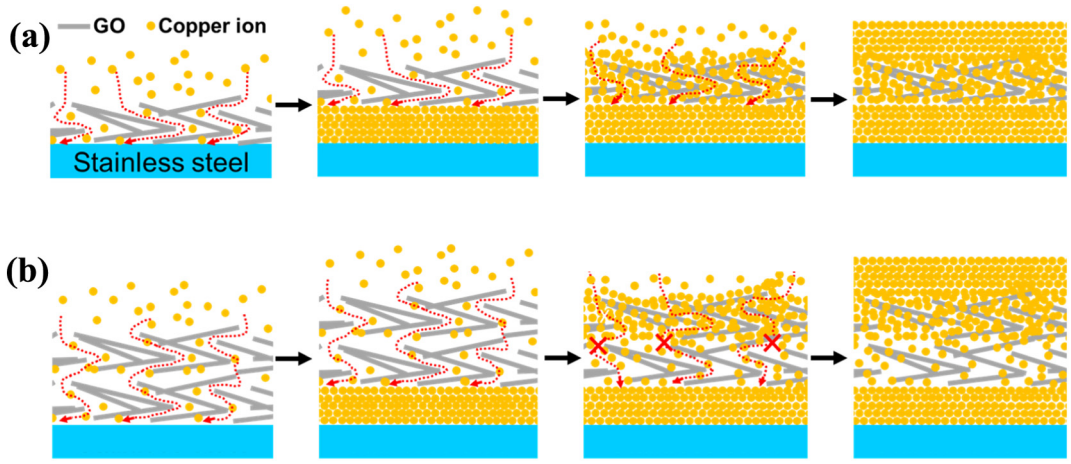

Fig. 10. Schematic diagram of the Cu/Gr/Cu foil formation. (a) Cu/Gr1/Cu with thinner Gr interlayer; (b) Cu/Gr2/Cu foil with relatively thicker Gr interlayer.

used in the areas, such as the Cu clad plate (CCL), printed circuit board (PCB), and lithium ion battery cathode collector system for saving row material and also the space.

4) This work introduces a new idea for preparing the layered composites via electrochemical process, and it can be applied in other materials.

CRediT authorship contribution statement

Gongsheng Song: Conceptualization, Formal analysis, Investigation, Methodology, Writing - original draft. **Qing Wang:** Writing - review & editing. **Li Sun:** Visualization. **Sishi Li:** Data curation. **Yafei Sun:** Funding acquisition, Resources. **Qiang Fu:** Software. **Chunxu Pan:** Project administration, Supervision, Validation, Resources, Writing - review & editing.

Declaration of competing interest

The authors declare that they have no known competing financial interests or personal relationships that could have appeared to influence the work reported in this paper.

Acknowledgment

This work was supported by the Suzhou Science and Technology Project (Prospective Application Research Program, No. SYG201740) and The Natural Science Foundation of Guangdong Province of China (No. 2015A030313591). The authors would like to acknowledge the Center for Electron Microscopy at Wuhan University for substantial supports to TEM work.

Appendix A. Supplementary data

Supplementary data to this article can be found online at https://doi.org/10.1016/j.matdes.2020.108629.

References

[1] H.-C. Chu, H.-Y. Tuan, High-performance lithium-ion batteries with 1.5 μm thin copper nanowire foil as a current collector, J. Power Sources 346 (2017) 40–48, https://doi.org/10.1016/j.jpowsour.2017.02.041.
[2] X. Ma, Z. Liu, H. Chen, Facile and scalable electrodeposition of copper current collectors for high-performance Li-metal batteries, Nano Energy 59 (2019) 500–507.
[3] S. Yuan, X.-l. Huang, D.-l. Ma, H.-g. Wang, F.-z. Meng, X.-b. Zhang, Engraving copper foil to give large-scale binder-free porous CuO arrays for a high-performance sodium-ion battery anode, Adv. Mater. 26 (2014) 2273–2279.
[4] M.-H. Yen, J.-H. Liu, J.-M. Song, S.-C. Lin, Electrochemical corrosion properties of commercial ultra-thin copper foils, J. Electron. Mater. 46 (2017) 5150–5157, https://doi.org/10.1007/s11664-017-5517-6.
[5] T. Chang, Y. Jin, L. Wen, C. Zhang, C. Leygraf, I.O. Wallinder, J. Zhang, Synergistic effects of gelatin and convection on copper foil electrodeposition, Electrochim. Acta 211 (2016) 245–254, https://doi.org/10.1016/j.electacta.2016.06.051.
[6] M. Eslami, H. Saghafian, F. Golestani-fard, A. Robin, Effect of electrodeposition conditions on the properties of Cu–Si3N4 composite coatings, Appl. Surf. Sci. 300 (2014) 129–140, https://doi.org/10.1016/j.apsusc.2014.02.021.
[7] M. Xu, H.D. Dewald, Impedance studies of copper foil and graphite-coated copper foil electrodes in lithium-ion battery electrolyte, Electrochim. Acta 50 (2005) 5473–5478, https://doi.org/10.1016/j.electacta.2005.03.051.
[8] M. Zhou, Y. Mai, H. Ling, F. Chen, W. Lian, X. Jie, Electrodeposition of CNTs/copper composite coatings with enhanced tribological performance from a low concentration CNTs colloidal solution, Mater. Res. Bull. 97 (2018) 537–543, https://doi.org/10.1016/j.materresbull.2017.09.062.
[9] X. Wang, B. Guo, S. Ni, J. Yi, M. Song, Acquiring well balanced strength and ductility of Cu/CNTs composites with uniform dispersion of CNTs and strong interfacial bonding, Mater. Sci. Eng. A 733 (2018) 144–152, https://doi.org/10.1016/j.msea.2018.07.046.
[10] G. Song, Z. Wang, Y. Gong, Y. Yang, Q. Fu, C. Pan, Direct determination of graphene amount in electrochemical deposited Cu-based composite foil and its enhanced mechanical property, RSC Adv. 7 (2017) 1735–1742, https://doi.org/10.1039/c6ra25512d.
[11] J. Li, P. Zhang, H. He, B. Shi, Enhanced the thermal conductivity of flexible copper foil by introducing graphene, Mater. Des. 187 (2020), 108373. https://doi.org/10.1016/j.matdes.2019.108373.
[12] A.K. Geim, K.S. Novoselov, The rise of graphene, Nat. Mater. 6 (2007) 183–191, https://doi.org/10.1038/nmat1849.
[13] K.S. Nooselov, A.K. Geim, S.V. Morozov, D. Jiang, Y. Zhang, S.V. Dubonos, I.V. Grigorieva, A.A. Firsov, Electric field effect in atomically thin carbon films, Science 306 (2004) 666–669, https://doi.org/10.1126/science.1102896.
[14] K.S. Novoselov, V.I. Fal Ko, L. Colombo, P.R. Gellert, M.G. Schwab, K. Kim, A roadmap for graphene, Nature 490 (2012) 192–200, https://doi.org/10.1038/nature11458.
[15] A.K. Geim, Graphene: status and prospects, Science 324 (2009) 1530–1534, https://doi.org/10.1126/science.1158877.
[16] F.M. Zhang, J. Wang, T.F. Liu, C.Y. Shang, Enhanced mechanical properties of few-layer graphene reinforced titanium alloy matrix nanocomposites with a network architecture, Mater. Des. 186 (2020), 108330. https://doi.org/10.1016/j.matdes.2019.108330.
[17] K. Jagannadham, Electrical conductivity of copper-Cgraphene composite films synthesized by electrochemical deposition with exfoliated graphene platelets, J. Vac. Sci. Technol. B 30 (2012) 03D109, https://doi.org/10.1007/s11663-011-9597-z.
[18] G. Song, Y. Yang, Q. Fu, C. Pan, Preparation of Cu-Graphene composite thin foils via DC electro-deposition and its optimal conditions for highest properties, J. Electrochem. Soc. 164 (2017) D652–D659, https://doi.org/10.1149/2.0121712jes.
[19] Y.J. Mai, M.P. Zhou, H.J. Ling, F.X. Chen, W.Q. Lian, X.H. Jie, Surfactant-free electrodeposition of reduced graphene oxide/copper composite coatings with enhanced wear resistance, Appl. Surf. Sci. 433 (2018) 232–239, https://doi.org/10.1016/j.apsusc.2017.10.014.
[20] G. Huang, H. Wang, P. Cheng, H. Wang, B. Sun, S. Sun, C. Zhang, M. Chen, G. Ding, Preparation and characterization of the graphene-Cu composite film by electrodeposition process, Microelectron. Eng. 157 (2016) 7–12, https://doi.org/10.1016/j.mee.2016.02.006.
[21] C.L. Pavithra, B.V. Sarada, K.V. Rajulapati, T.N. Rao, G. Sundararajan, A new electrochemical approach for the synthesis of copper-graphene nanocomposite foils with high hardness, Sci. Rep. 4 (2014) 4049, https://doi.org/10.1038/srep04049.
[22] Y. Kim, J. Lee, M.S. Yeom, J.W. Shin, H. Kim, Y. Cui, J.W. Kysar, J. Hone, Y. Jung, S. Jeon, S.M. Han, Strengthening effect of single-atomic-layer graphene in metal˙Cgraphene nanolayered composites, Nat. Commun. 4 (2013) https://doi.org/10.1038/ncomms3114.

[23] J.M. Tao, X.F. Chen, P. Hong, J.H. Yi, Microstructure and electrical conductivity of laminated Cu/CNT/Cu composites prepared by electrodeposition, J. Alloys Compd. 717 (2017) 232–239, https://doi.org/10.1016/j.jallcom.2017.05.074.
[24] B.T.J. Kang, J.W. Yoon, D.I. Kim, S.S. Kum, Y.H. Huh, J.H. Hahn, S.H. Moon, H.Y. Lee, Y.H. Kim, Sandwich-type laminated nanocomposites developed by selective dip-coating of carbon nanotubes, Adv. Mater. 19 (2007) 427–432, https://doi.org/10.1002/adma.200600908.
[25] S. Chen, H. Xu, X. Luo, X. Qin, Z. Han, Discuss on processing difficulties of ultra-thin copper foil in PCB manufacturing, Printed circuit information 4 (2013)(197-191, In Chinese).
[26] G.F. Deng, G.R. He, J.Q. Huang, P. Xu, Influence of rare earth on the peeling properties of ultra-thin copper foil with carrier, Adv. Mater. Res. 652–654 (2013) 1755–1758, https://doi.org/10.4028/www.scientific.net/AMR.652-654.1755.
[27] J.A. Quezada-Rentería, L.F. Cházaro-Ruiz, J.R. Rangel-Mendez, Synthesis of reduced graphene oxide (rGO) films onto carbon steel by cathodic electrophoretic deposition: anticorrosive coating, Carbon 122 (2017) 266–275, https://doi.org/10.1016/j.carbon.2017.06.074.
[28] B.P. Singh, S. Nayak, K.K. Nanda, B.K. Jena, S. Bhattacharjee, L. Besra, The production of a corrosion resistant graphene reinforced composite coating on copper by electrophoretic deposition, Carbon 61 (2013) 47–56, https://doi.org/10.1016/j.carbon.2013.04.063.
[29] M. Diba, A. García-Gallastegui, R.N. Klupp Taylor, F. Pishbin, M.P. Ryan, M.S.P. Shaffer, A.R. Boccaccini, Quantitative evaluation of electrophoretic deposition kinetics of graphene oxide, Carbon 67 (2014) 656–661, https://doi.org/10.1016/j.carbon.2013.10.041.
[30] M. Diba, D.W.H. Fam, A.R. Boccaccini, M.S.P. Shaffer, Electrophoretic deposition of graphene-related materials: a review of the fundamentals, Prog. Mater. Sci. 82 (2016) 83–117, https://doi.org/10.1016/j.pmatsci.2016.03.002.
[31] D.B. Xiong, M. Cao, Q. Guo, Z. Tan, G. Fan, Z. Li, D. Zhang, Graphene-and-copper artificial nacre fabricated by a preform impregnation process: bioinspired strategy for strengthening-toughening of metal matrix composite, ACS Nano 9 (2015) 6934–6943, https://doi.org/10.1021/acsnano.5b01067.
[32] K. Chu, F. Wang, Y.-b. Li, X.-h. Wang, D.-j. Huang, H. Zhang, Interface structure and strengthening behavior of graphene/CuCr composites, Carbon 133 (2018) 127–139, https://doi.org/10.1016/j.carbon.2018.03.018.
[33] K. Chu, X.-h. Wang, F. Wang, Y.-b. Li, D.-j. Huang, H. Liu, W.-l. Ma, F.-x. Liu, H. Zhang, Largely enhanced thermal conductivity of graphene/copper composites with highly aligned graphene network, Carbon 127 (2018) 102–112, https://doi.org/10.1016/j.carbon.2017.10.099.
[34] Y. Zhu, S. Murali, W. Cai, X. Li, J.W. Suk, J.R. Potts, R.S. Ruoff, Graphene and graphene oxide: synthesis, properties, and applications, Adv. Mater. 22 (2010) 3906–3924, https://doi.org/10.1002/adma.201001068.
[35] Z.T. Luo, Y. Lu, L.A. Somers, A.T.C. Johnson, High yield preparation of macroscopic graphene oxide membranes, J. Am. Chem. Soc. 131 (2009) https://doi.org/10.1021/ja807934n(898-+).
[36] A.C. Ferrari, J.C. Meyer, V. Scardaci, C. Casiraghi, M. Lazzeri, F. Mauri, S. Piscanec, D. Jiang, K.S. Novoselov, S. Roth, A.K. Geim, Raman spectrum of graphene and graphene layers, Phys. Rev. Lett. 97 (2006), 187401. https://doi.org/10.1103/PhysRevLett.97.187401.
[37] A.C. Ferrari, D.M. Basko, Raman spectroscopy as a versatile tool for studying the properties of graphene, Nat. Nanotechnol. 8 (2013) 235–246, https://doi.org/10.1038/nnano.2013.46.
[38] M.S. Dresselhaus, A. Jorio, M. Hofmann, G. Dresselhaus, R. Saito, Perspectives on carbon nanotubes and graphene Raman spectroscopy, Nano Lett. 10 (2010) 751–758, https://doi.org/10.1021/nl904286r.
[39] G. Chai, Y. Sun, J.J. Sun, Q. Chen, Mechanical properties of carbon nanotube-copper nanocomposites, J. Micromech. Microeng. 18 (2008) 035013, https://doi.org/10.1088/0960-1317/18/3/035013.
[40] K. Chu, F. Wang, X.H. Wang, Y.B. Li, Z.R. Geng, D.J. Huang, H. Zhang, Interface design of graphene/copper composites by matrix alloying with titanium, Mater. Des. 144 (2018) 290–303, https://doi.org/10.1016/j.matdes.2018.02.038.
[41] S. Zhang, P. Huang, F. Wang, Graphene-boundary strengthening mechanism in Cu/graphene nanocomposites: a molecular dynamics simulation, Mater. Des. 190 (2020), 108555. https://doi.org/10.1016/j.matdes.2020.108555.
[42] G. Xie, M. Forslund, J. Pan, Direct electrochemical synthesis of reduced graphene oxide (rGO)/copper composite films and their electrical/electroactive properties, ACS Appl. Mater. Interfaces 6 (2014) 7444–7455, https://doi.org/10.1021/am500768g.
[43] X. Zhang, C. Shi, E. Liu, N. Zhao, C. He, Effect of interface structure on the mechanical properties of graphene nanosheets reinforced copper matrix composites, ACS Appl. Mater. Interfaces 10 (2018) 37586–37601, https://doi.org/10.1021/acsami.8b09799.
[44] E. Gao, Y. Cao, Y. Liu, Z. Xu, Optimizing interfacial cross-linking in graphene-derived materials, which balances Intralayer and interlayer load transfer, ACS Appl. Mater. Interfaces 9 (2017) 24830–24839, https://doi.org/10.1021/acsami.7b04411.
[45] X. Chen, J. Tao, Y. Liu, R. Bao, F. Li, C. Li, J. Yi, Interface interaction and synergistic strengthening behavior in pure copper matrix composites reinforced with functionalized carbon nanotube-graphene hybrids, Carbon 146 (2019) 736–755, https://doi.org/10.1016/j.carbon.2019.02.048.
[46] G. Song, S. Li, G. Liu, Q. Fu, C. Pan, Influence of graphene oxide content on the Zn-Gr composite layer prepared by pulse reverse electro-plating, J. Electrochem. Soc. 165 (2018) D501–D510, https://doi.org/10.1149/2.0431811jes.
[47] L. Zheng, H. Zheng, D. Huo, F. Wu, L. Shao, P. Zheng, Y. Jiang, X. Zheng, X. Qiu, Y. Liu, Y. Zhang, N-doped graphene-based copper nanocomposite with ultralow electrical resistivity and high thermal conductivity, Sci. Rep. 8 (2018) 9248, https://doi.org/10.1038/s41598-018-27667-9.
[48] S.J. Kim, D.H. Shin, Y.S. Choi, H. Rho, M. Park, B.J. Moon, Y. Kim, S.K. Lee, D.S. Lee, T.W. Kim, S.H. Lee, K.S. Kim, B.H. Hong, S. Bae, Ultrastrong graphene-copper core-shell wires for high-performance electrical cables, ACS Nano 12 (2018) 2803–2808, https://doi.org/10.1021/acsnano.8b00043.
[49] R. Mehta, S. Chugh, Z. Chen, Enhanced electrical and thermal conduction in graphene-encapsulated copper nanowires, Nano Lett. 15 (2015) 2024–2030, https://doi.org/10.1021/nl504889t.
[50] M. Cao, Y. Luo, Y. Xie, Z. Tan, G. Fan, Q. Guo, Y. Su, Z. Li, D.B. Xiong, The influence of interface structure on the electrical conductivity of graphene embedded in aluminum matrix, Adv. Mater. Interfaces (2019) 1900468, https://doi.org/10.1002/admi.201900468.
[51] W. Li, D. Li, Q. Fu, C. Pan, Conductive enhancement of copper/graphene composites based on high-quality graphene, RSC Adv. 5 (2015) 80428–80433, https://doi.org/10.1039/c5ra15189a.